Paramagnetic Resonance Line Shapes of Fe^{++} in MgO†

D. H. McMahon*
Laboratory of Atomic and Solid State Physics and Department of Physics, Cornell University, Ithaca, New York
(Received 18 October 1963)

The asymmetric $\Delta M=2$ paramagnetic resonance line shapes of Fe^{++} in MgO are explained using a model of stochastic distributions of cartesian strain components as a strain-broadening mechanism. Strains broaden the $\Delta M=2$ resonances at lower frequencies by means of a direct zero-field splitting and at higher frequencies by means of a strain-induced change in g value. It is found that this model of broadening gives mathematical expressions for the $\Delta M=2$ line shapes which agree quantitatively with experimental results.

INTRODUCTION

THE paramagnetic resonance spectrum of Fe^{++} in MgO consists of 3 lines: One transition is very broad and represents the normal $\Delta M=1$ transition; the other two are forbidden $\Delta M=2$ transitions and exhibit narrower asymmetric line shapes. Originally, Low[1] suggested the possibility of strain broadening as a line-shape mechanism. Watkins and Feher[2] have since measured the effects of applied uniaxial strains of the paramagnetic resonance spectrum, showing that the Fe^{++} ion is sensitive to strains and making the strain-induced linewidth hypothesis more reasonable. Feher and Weger[3] have applied the concept of random internal stress components to make a second-moment calculation of the strain-broadened resonance of Mn^{++} and Fe^{+++} in MgO. One can also apply the concept of stochastic distributions of strain components to make a calculation of the line shape itself. This procedure, though less rigorous than a calculation of moments, can be applied with benefit to the Fe^{++} $\Delta M=2$ resonance lines because it explains the asymmetric shapes, because it permits a quantitative comparison of the $\Delta M=2$ and $\Delta M=1$ shapes, and because the calculation of moments does not apply.

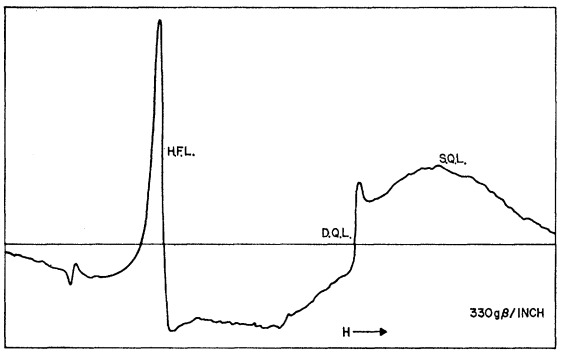

FIG. 1. The paramagnetic resonance spectrum of Fe^{++} in MgO at 9.5 Gc/sec. The derivative signal is illustrated.

One finds at low frequencies that the paramagnetic resonances are strain broadened by means of a direct zero-field splitting mechanism which can be adequately explained using the spin-strain Hamiltonian of Watkins.[2] However, at higher frequencies, a g distribution broadening mechanism predominates and it must be taken into account to explain line shape changes.

The paramagnetic resonance spectrum of Fe^{++} in MgO is shown in Fig. 1. The broad line at $g=3.4$ is the usual $\Delta M=1$ transition. The width of this transition, which will be referred to as the "single quantum line" and abbreviated SQL, is accounted for by the extreme sensitivity of Fe^{++} to strains.

The narrow line at $g=3.4$ is, in terms of perturbation theory, a second-order process in which two microwave photons are absorbed by the spin in rapid succession. This transition takes place between the two end levels of the ground-state triplet. Its width is less because it is broadened only by second-order strain shifts and because the energy denominator of second-order rf perturbation makes the process likely only when the first-order strain shift is small. This type of transition is generally called a "double quantum transition" and will be abbreviated DQL.

The line at $g=6.8$ is called the "half-field line" and abbreviated HFL. This transition, which is strictly forbidden for cubic crystal fields, occurs because strains produce small admixtures of the pure Zeeman eigenfunctions. Using the admixture of eigenfunctions, the rf field can induce a transition between the two end levels of the triplet ground state using only one photon.

The DQL and HFL will be collectively referred to as $\Delta M=2$ transitions. Low[1] has given the above interpretation for the HFL Orton *et al.*[4] have established the double quantum nature of a Ni^{++} transition in MgO, a case which is similar to Fe^{++} in MgO.

THEORY OF STRAIN-INDUCED LINE SHAPES

It will be assumed from the beginning that strains, caused by nearby crystal imperfections, are the cause of the observed line shapes and a theory based on this premise will be developed. The results of experiments presented later on will justify this assumption.

† Supported by U. S. Atomic Energy Commission and the Alfred P. Sloan Foundation.
* Present address: Sperry Rand Research Center, Sudbury, Massachusetts.
[1] W. Low, *Paramagnetic Resonance in Solids* (Academic Press Inc., New York, 1960).
[2] G. Watkins and E. Feher, Bull. Am. Phys. Soc. **7**, 29 (1962).
[3] E. Feher and M. Weger, Bull. Am. Phys. Soc. **7**, 613 (1962).
[4] J. W. Orton, P. Auzins, and J. E. Wertz, Phys. Rev. Letters 4, 128 (1960).

It is likely that the observed strain broadening of the Fe^{++} resonance lines is due to dislocations. The strain fields produced by dislocations are in general anisotropic; dislocations are preferentially oriented, and often form nets of dislocations resembling a superlattice structure. Not only is the problem of calculating line shapes in terms of a dislocation model too difficult to treat mathematically, even if the dislocation structure were known, but, in addition, one does not know such essential details as whether the Fe^{++} ions are randomly distributed in the lattice. It is therefore not reasonable to attempt to explain line shapes from first principles using a dislocation model.

An alternate, more modest approach, is to explain the HFL and DQL widths and shapes in terms of information obtained from the SQL. Assume that there is a stochastic distribution in the values of the strain components e_{xx}, e_{xy}, etc. at the paramagnetic ions sites. If the set of 6 independent Cartesian strain components is known, one may use Watkins' effective spin-strain interaction to determine completely the effect of the strain components of the spin system. Having determined the resonance energy shifts in terms of the strain components, the strain induced line shape is calculated by integrating over the probability distribution of strain components. The type of probability distribution is chosen so that the shape of the SQL agrees with the experimentally observed Lorentzian line shape.

If the static magnetic field is along the [100] axis of the crystal, the spin-strain interaction can be written in matrix form, that is, in a representation in which S_z is diagonal. The result is

$$\begin{vmatrix} (-G_{11}/4)(e_{xx}+e_{yy}-2e_{zz}) & (G_{44}/)\sqrt{2}(e_{xy}-ie_{yz}) & (3G_{11}/4)(e_{xx}-e_{yy})-iG_{44}e_{xy} \\ (G_{44}/\sqrt{2})(e_{xy}+ie_{yz}) & (2G_{11}/4)(e_{xx}+e_{yy}-2e_{zz}) & (-G_{44}/\sqrt{2})(e_{xz}-ie_{yz}) \\ (3G_{11}/4)(e_{xx}-e_{yy})+iG_{44}e_{xy} & (-G_{44}/\sqrt{2})(e_{xz}+ie_{yz}) & (-G_{11}/4)(e_{xx}+e_{yy}-2e_{zz}) \end{vmatrix}.$$

Changing the orientation of the crystal relative to the static magnetic field will intermix the diagonal and off-diagonal elements of this array and produce minor changes in the width of the Fe^{++} paramagnetic resonance lines. These changes are not of interest here, and consequently the theoretical analysis and experimental procedure are carried out only for the case in which the magnetic field is along a [100] crystal direction. Watkins[2] and Shiren,[5] using different techniques, have determined the constants of this Hamiltonian. The average of their results is

$$G_{11}(=-2G_{12})=720\ \text{cm}^{-1},\quad G_{44}=460\ \text{cm}^{-1}.$$

This interaction is applied as a perturbation assuming that the three levels of the ground state are already split by a relatively large Zeeman energy. From this one can deduce that the resonance condition of the SQL in the presence of strains is,

$$E=\hbar\omega_0\pm(\tfrac{3}{4})G_{11}(e_{xx}+e_{yy}-2e_{zz})+\text{2nd-order terms}.$$

Correspondingly, the resonance condition for the DQL is

$$E=\hbar\omega_0+(G_{44}^2/\hbar\omega_0)(e_{xy}^2+e_{yz}^2+e_{zx}^2)+(9G_{11}^2/16\hbar\omega_0)(e_{xx}-e_{yy})^2.$$

In these two cases $\hbar\omega_0$ is the Zeeman energy between two adjacent levels. The resonance condition for the HFL is

$$E=\hbar\omega_0+(2G_{44}^2/\hbar\omega_0)(e_{xy}^2+e_{yz}^2+e_{zx}^2)+(9G_{11}^2/8\hbar\omega_0)(e_{xx}-e_{yy})^2.$$

Here, as in subsequent applications referring to the HFL, $\hbar\omega_0$ is the Zeeman energy between the two end states of the triplet. This formulation is consistent with the fact that paramagnetic spectrometers are constant frequency devices. The difference in the DQL and HFL resonating conditions occurs because two rf photons are absorbed in the former and one in the latter.

Since the HFL is forbidden in a perfectly cubic field, the strength of the rf field interaction is strain dependent. One must therefore calculate the strength of the interaction in terms of the strain components. If one denotes ϕ_+, ϕ_0, ϕ_- as the Zeeman eigenfunctions in the absence of strains, the eigenfunctions in the presence of strains are,

$$\Phi_+=\phi_+ + \frac{G_{44}}{\sqrt{2}}\frac{(e_{xz}+ie_{yz})}{\hbar\omega_0/2}\phi_0+(\quad)\phi_-,$$

$$\Phi_-=\phi_- + \frac{G_{44}}{\sqrt{2}}\frac{(e_{xz}-ie_{yz})}{\hbar\omega_0/2}\phi_0+(\quad)\phi_+.$$

Since the rf field interaction can be represented as $\mathrm{H}_{\mathrm{rf}}=gbH_x(S_++S_-)$, the magnitude of the interaction for the HFL is

$$\mathfrak{IC}_{\mathrm{hf}}=\langle\Phi_+|\mathfrak{IC}_{\mathrm{rf}}|\Phi_-\rangle=2\sqrt{2}G_{44}\frac{(e_{xz}-ie_{yz})}{\hbar\omega_0}\mathfrak{IC}_{\mathrm{rf}}.$$

Assume that the distribution of Cartesian strain components is given by the probability $P(e)=P(e_{xx}, e_{yy}, e_{zz}, e_{yz}, e_{zx}, e_{xy})$ of finding a spin subjected to the strains e_{xx}, e_{yy}, etc. To make practical use of the distribution in solving problems, it is assumed to be separable into products of probability distributions of individual strain components,

$$P(e)=P(e_{xx})P(e_{yy})P(e_{zz})P(e_{xy})P(e_{yz})P(e_{zx}).$$

[5] N. S. Shiren, Bull. Am. Phys. Soc. 7, 29 (1962).

Since it is known that the SQL has a Lorentzian shape within errors of measurement, one must choose the distributions of strain to be Lorentzian in order that the SQL be Lorentzian. (Gaussian distributions give a Gaussian shaped SQL.) The choice of Lorentzian instead of near-Lorentzian distributions is for mathematical convenience.

Because of symmetry considerations, one can assume that all of the widths of the distributions of diagonal strains are the same and that all of the widths of the distributions of off-diagonal strains are the same. Therefore one has,

$$P(e_{ii})=\frac{\Delta}{\pi}\frac{1}{e_{ii}^2+\Delta^2};\quad P(e_{ij})=\frac{\delta}{\pi}\frac{1}{e_{ij}^2+\delta^2},\quad i\neq j,$$

where Δ and δ are the widths of the diagonal and off-diagonal distributions of strain, respectively.

CALCULATION OF LINE SHAPES

The procedure for calculating the strain-induced line shapes will be as follows. First of all, the power absorbed for one spin as a function of the Cartesian strain components is found. The power absorbed by one spin will have a strain-shifted resonance denominator of width T_2^{-1}. This finite width, over which a spin can absorb power, will be replaced by a Dirac delta function resonating condition. The delta function resonating condition, which is a function of the strain components, is integrated over the probability of finding a given set of strain components, producing a result which is equivalent to summing over an ensemble of spins. Because the delta function and its associated factors represent power absorbed per spin, the result of integrating over the strain probabilities gives a line shape that represents total rf power absorbed as a function of frequency.

In Appendix 1, formulas for the absorbed power per spin as a function of frequency and strain are derived using the density matrix approach. The results of this Appendix can be summarized as,

$$R_{\rm sq}=\frac{4}{3}\frac{\hbar\omega_0 S\tau}{T_1}\frac{1}{1+T_2^2(\omega+\omega_1)^2},$$

$$R_{\rm dq}=\frac{8\hbar\omega_0 S^2\tau}{T_1}\times\frac{1}{[1+T_2^2(\omega+\omega_1+\omega_2')^2][1+T_2^2(\omega-\omega_1+\omega_2')^2]},$$

$$R_{\rm hf}=\frac{4}{3}\frac{\hbar\omega_0 S'\tau}{T_1}\frac{8(e_{xz}^2+e_{yz}^2)}{\hbar\omega_0^2}\frac{1}{1+T_2^2(\omega+\omega_2)^2},$$

where ω=rf frequency measured with respect to zero-strain resonance frequency

$\omega_1=\frac{3}{4}G_{11}(e_{xx}+e_{yy}-2e_{zz})$

=1st-order perturbation strain shift,

$$\omega_2=\frac{2G_{44}^2}{\hbar\omega_0}(e_{xy}^2+e_{yz}^2+e_{zx}^2)+\frac{9}{8}\frac{G_{11}^2}{\hbar\omega_0}(e_{xx}-e_{yy})^2$$

=2nd-order strain shift for HFL,

$$\omega_2'=\frac{G_{44}^2}{\hbar\omega_0}(e_{xy}^2+e_{yz}^2+e_{zx}^2)+\frac{9}{16}\frac{G_{11}^2}{\hbar\omega_0}(e_{xx}-e_{yy})^2$$

=2nd-order strain shift for DQL,

$S=g^2\beta^2H_1^2T_1T_2$=saturation factor SQL and DQL,

$S'=g^2\beta^2H_1^2T_1'T_2$=saturation factor for HFL.

Note that the g in S' is the same as the g in S. This occurs because the strength of the rf matrix element for the HFL was calculated in terms of the rf matrix element of the SQL.

Replacing the finite widths of the resonating denominators by an infinitely sharp δ function amounts to the following replacement in an integrand:

$$\frac{1}{1+T_2^2(\omega-\omega_1)^2}\rightarrow\frac{\pi}{T_2}\delta(\omega-\omega_1)=\frac{\pi\hbar}{T_2}\delta(E-E_1).$$

Changing the frequency to energy units will be convenient later on.

This substitution is justified if the intensity of the line does not change significantly in a frequency interval $\Delta\omega\simeq T_2^{-1}$, a condition which is always satisfied for the SQL and which is usually satisfied for the HFL. On the other hand, it will be found that this replacement is not a particularly good assumption for the DQL because in this approximation the DQL shows a discontinuous derivative. It does, however, produce a simplification that allows one to perform the calculation and one can in fact get good qualitative results for the DQL by adding T_2 as a broadening mechanism at the end of the calculation.

The method of distributions of strains consists of entering the R's in an integrand which is summed over the probability distributions of strains. Thus one has, when substituting in the appropriate δ functions,

$$I(E)_{\rm sq}=\frac{4\pi\hbar\omega_0}{3}\frac{(g\beta H_{\rm rf})^2\tau}{\hbar}\int\delta(E-E_1)P(E_1)dE_1,$$

$$I(E)_{\rm hf}=\frac{4\pi}{3}\hbar\omega_0\frac{(g\beta H_{\rm rf})^2\tau}{\hbar}\int\frac{8(e_{xz}^2+e_{yz}^2)}{(\hbar\omega_0)^2}\times\delta(E-E_2)P(E_2)dE_2,$$

$$I(E)_{dq}=8\pi\hbar\omega_0(g^2\beta^2H_{rf}^2)^2\tau T_1 \times\int\delta(E_1)\,\delta(E-E_2)P(E_1,E_2)dE_1dE_2,$$

where

$$P(E_1)=\int\delta[E_1-G_{11}(e_{xx}+e_{yy}-2e_{zz})]P(e)de,$$

$$P(E_2)=\int\delta\left[E_2-\frac{2G_{44}^2}{\hbar\omega_0}(e_{xy}^2+e_{yz}+e_{zx}^2) -\frac{9}{8}\frac{G_{11}^2}{\hbar\omega_0}(e_{xx}-e_{yy})^2\right]P(e)de,$$

$$P(E_1E_2)=\int\delta[E_1-G_{11}(e_{xx}+e_{yy}-2e_{zz})] \times\delta\left[E_2-\frac{G_{44}^2}{\hbar\omega_0}(e_{xy}^2+e_{yz}^2+e_{zx}^2) -\frac{9}{16}\frac{G_{11}^2}{\hbar\omega_0}(e_{xx}-e_{yy})^2\right]P(e)de,$$

$$P(e)=\left(\frac{\Delta}{\pi}\right)^3\left(\frac{\delta}{\pi}\right)^3\frac{1}{(e_{xx}^2+\Delta^2)}\frac{1}{(e_{yy}^2+\Delta^2)}\frac{1}{(e_{zz}^2+\Delta^2)} \times\frac{1}{(e_{xy}^2+\delta^2)}\frac{1}{(e_{yz}^2+\delta^2)}\frac{1}{(e_{zx}^2+\delta^2)},$$

$$de=de_{xx}de_{yy}de_{zz}de_{xy}de_{yz}de_{zx}.$$

In Appendix 2, the evaluation of the above integrals was carried out as far as possible in terms of closed form expressions. The result is

$$I(E)_{sq}=\frac{4\pi}{3}\hbar\omega_0\frac{(g\beta H_{rf})^2}{\hbar}\tau\frac{3G_{11}\Delta}{\pi}\frac{1}{E^2+(3G_{11}\Delta)^2}, \quad (1)$$

$$I(E)_{hf}=\frac{4\pi}{3}\hbar\omega_0\frac{(g\beta H_{rf})^2}{\hbar}\tau\left(\frac{16}{3\pi^3}\times\frac{ba^{1/2}}{\hbar\omega_0}\right) \times\int_0^1\frac{dyH(b/y)}{y(1-y+a)(1-y)^{1/2}},$$

with

$$H(b/y)=\int_0^1\frac{dx}{[x^2+(b/y)][1-x^2+(b/y)]^{1/2}[1-x^2+(2b/y)]}$$

and

$$a=\frac{2[(8/3)G_{11}\Delta]^2}{\hbar\omega_0E}, \quad b=\frac{2\delta^2G_{44}^2}{\hbar\omega_0E}, \quad (2)$$

$$I(E)_{dq}=8\pi\hbar\omega_0(g\beta H_{rf})^2T_1\tau\left(\frac{6}{\pi^2}\frac{1}{\epsilon n^2}b_1^2a_1^{3/2}\right) \times\int_0^1\frac{dyH(b_1/y)}{y^2(1-y)^{1/2}(1-y+4a_1)(1-y+a_1)} \quad (3)$$

with

$$H(b_1/y)=\int_0^1\frac{dx}{[x^2+(b_1/y)][1-x^2+(b_1/y)]^{1/2}[1-x^2+(2b_1/y)]}$$

and

$$a_1=\frac{[(8/3)\Delta G_{11}]^2}{\hbar\omega_0E}, \quad b_1=\frac{\delta^2G_{44}^2}{\hbar\omega_0E},$$

$$\epsilon=(4/3)G_{11}\Delta, \quad n=G_{44}\delta.$$

Graphs of the functions $I(E)_{hf}$ and $I(E)_{dq}$ have been obtained using a computer program to evaluate the integrals. The results, plotted in terms of the dimensionless variables $(1/a)=9E\hbar\omega_0/128G_{11}^2\Delta^2$ and $(1/a_1)=(2/a)$, are shown in Figs. 2 and 3. Even though the width depends on the ratio a/b, the shapes are insensitive to the ratio and hence only the case $a=b$ is shown.

The HFL and DQL shapes are broad and have relatively steep slopes at the high-field or zero-strain side of the lines. Because of this, the derivatives of the line shapes are significantly different from zero only for small strains and the derivatives are asymmetric. Another characteristic common to these resonances is that they get narrower as the spectrometer frequency is increased because they scale according to the factor $1/a$ or $1/a_1$ as the case may be.

The line shapes are not valid for large $1/a$ because the theory does not take into account the fact that imperfections can not be nearer the paramagnetic ions than nearest-neighbor sites.

HEIGHT AND WIDTH COMPARISONS OF SQL AND HFL

It is useful, in terms of comparing theory and experiment, to make a quantitative comparison of relative widths and heights using the above theory. Because the SQL and DQL intensities vary differently with rf power, a comparison of heights is not convenient in this case. As a result, height and width comparisons of the SQL and HFL will be made and the widths of the HFL and DQL will be compared.

For a paramagnetic spectrometer with linear detection the output voltage (deflection of recorder pen) is proportional to the derivative with respect to magnetic field of absorbed power divided by the rf magnetic field strength. If the rf power level at the sample cavity is held constant, the ratio of the absorbed power, that is, the ratio of the $I(E)$'s for the SQL and HFL, will yield a quantity which can be determined experimentally.

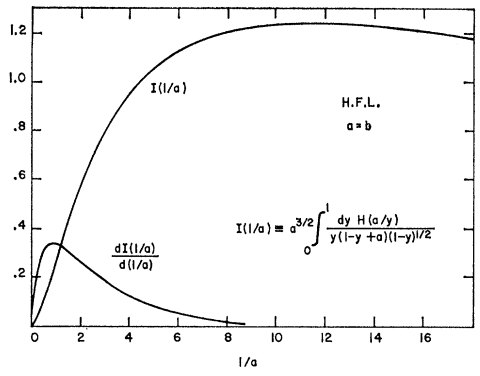

FIG. 2. The strain induced HFL shape at low frequencies assuming $a=b$. For comparison with experiment the derivative shape is included.

Since spectrometers plot out derivatives of line shapes, it will be convenient to express parameters in terms of the derivatives of the SQL and HFL. A computer program was used to calculate $dD(1/a)/d(1/a)$ versus $1/a$, where,

$$D\left(\frac{1}{a}\right)\equiv ba^{1/2}\int_0^1 \frac{dyH(b/y)}{y(1-y+a)(1-y)^{1/2}}$$

for the three cases $a=b$, $a=4b$, $4a=b$. The results are illustrated in Fig. 4. As convenient parameters for measuring the width and height of the HFL, the width at half the maximum height of the derivative, and the maximum height of the derivative will be used. These will be compared with the peak-to-peak height of the SQL derivative and the width of the SQL between the two peaks. From the graphs of the function $dD(1/a)/d(1/a)$, one gets the relationships (accurate to about 5%),

$$\left.\frac{dD(1/a)}{d(1/a)}\right|_{\max}=0.32\left(\frac{a}{b}\right)^{0.73},\qquad W_{\rm hf}=\frac{128G_{11}^2\Delta^2}{9\hbar\omega_0}3.0\left(\frac{b}{a}\right)^{0.84} \tag{4}$$

and

$$\left.\frac{dI(e)_{\rm hf}}{dE}\right|_{\max}=\left(\frac{4\pi\hbar\omega_0\tau g^2\beta^2H_{\rm rf}^2}{3\hbar}\right)\left(\frac{16}{3\pi^3\hbar\omega_0}\right)\times\left.\frac{dD(1/a)}{d(1/a)}\right|_{\max}\frac{d(1/a)}{dE}.$$

The peak-to-peak width and height of the SQL derivative are given by

$$\frac{dI(E)_{\rm sq}}{dE}=\left(\frac{4\pi\hbar\omega_0g^2\beta^2H_{\rm rf}^2\tau}{3\hbar}\right)\left(\frac{3\sqrt{3}}{4\pi}\right)\frac{1}{(3G_{11}\Delta)^2}.$$

$$W_{\rm sq}=2\sqrt{3}G_{11}\Delta.$$

In measuring heights, one determines the quantity

$$\Delta I=\left.\frac{dI(E)}{d(E)}\right|_{\max}M,$$

where M is the depth of the magnetic field modulation in energy units. Taking the ratio of the two height parameters, one gets

$$\frac{\Delta I_{\rm hf}}{\Delta I_{\rm sq}}=\frac{m_{\rm hf}}{m_{\rm sq}}0.17\left(\frac{a}{b}\right)^{0.73}, \tag{5}$$

where m represents the modulation depth in gauss.

Taking the ratio of the two widths, one finds, if $w_{\rm sq}$ and $w_{\rm hf}$ represent the widths in gauss and H_2 is the magnetic field for $g=2$, that,

$$H_2w_{\rm hf}/w_{\rm sq}^2=2.3(b/a)^{0.84}. \tag{6}$$

Some features brought out by the height and width comparisons are: The width of the HFL is proportional to the square of the SQL width and is inversely proportional to the spectrometer frequency (Zeeman splitting); the ratio of the heights of the derivative curves for the SQL and HFL is independent of frequency.

If one uses Figs. 2 and 3 to compare the half-height widths of the HFL and DQL, one gets the relation $2w_{\rm dq}=w_{\rm sq}$, where $w_{\rm dq}$ and $w_{\rm sq}$ are measured in gauss.

It is evident that the theory does not determine the value of the ratio a/b.

$M=2$ LINE SHAPE AT HIGHER FREQUENCIES

When the Fe^{++} $\Delta M=2$ resonances are observed using a high-frequency spectrometer (4-mm wavelength), a second-order perturbation through the next higher spin-orbit state, which can be schematically represented as

$$\frac{\text{(strain)(Zeeman interaction)}}{\text{(spin-orbit splitting)}},$$

is effective in producing another strain-broadening mechanism. This mechanism, because it depends on

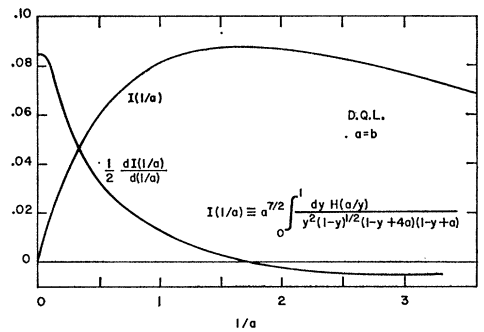

FIG. 3. The strain-induced DQL shape at low frequencies for the case $a=b$.

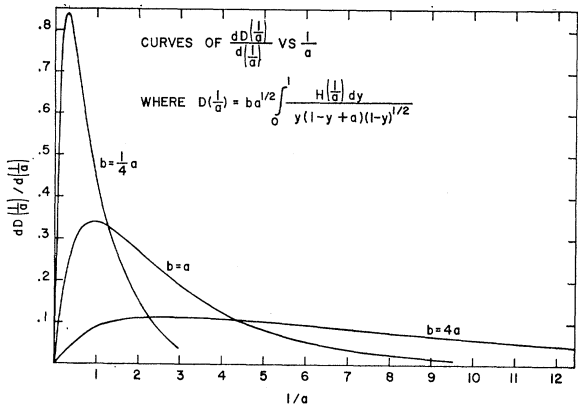

FIG. 4. The low-frequency HFL shape for different values of the ratio a/b.

the Zeeman interaction, represents a strain-induced g shift. The distribution of strains implies a distribution of g's and hence a linewidth.

Because excited states within a manifold of a spin-orbit multiplet are involved, the strain interaction must be expressed in terms of a more general orbital-strain interaction instead of the "effective spin" strain interaction used above. In order to calculate the size of the orbital-strain coupling constants, this same interaction in terms of orbital operators is applied as a perturbation between the ground-state triplet eigenfunctions. These eigenfunctions are expressed as products of spin and orbital operators and result from applying crystal field, spin-orbit, and Zeeman perturbations in succession to the ^5D free ion configuration of Fe^{++}. For the case of the ground state triplet levels, the magnitude of the orbital-strain coupling constants can then be found in terms of the equally applicable "effective spin" strain interaction, for which the coupling constants are known.

Using this procedure, one has for the relative energy shift between the $M_s=\pm 1$ ground states (caused by the g distribution perturbation):

$$\nabla=\frac{27\hbar\omega_0}{4\lambda}G_{11}(e_{xx}+e_{yy}-2e_{zz}),$$

where $\lambda(\mathbf{L}\cdot\mathbf{S})$ is the spin-orbit coupling.

The correct way of introducing the new width mechanism into the HFL is to include it as part of the energy shift factor in the δ function resonating condition. Thus one has,

$$I(E)_{\rm hf}=\left(\frac{4\hbar\omega_0\tau S'}{T_1'}\right)\int\frac{8(e_{xz}^2+e_{yz}^2)}{\hbar^2\omega_0^2}\times\delta[E-E_2(e)-\nabla(e)]P(e)de,$$

where $P(e)$, de, and E_2 are defined as in the HFL case above. This formula takes into account the fact that the new width mechanism enters only in the resonating frequency condition, but does not relax further the forbidden nature of the $\Delta M=2$ selection rule. Consequently, the transition probability matrix element of the HFL is still the same.

Unfortunately this formulation leads to mathematical difficulties which cannot be easily circumvented. An alternate and sufficiently accurate approach is to find the width of the distribution of ∇ as a function of energy position E produced by the low-frequency broadening mechanism. The unnormalized probability of finding the energy shift ∇ at E is

$$P(\nabla,E)=\int\delta[\nabla-E_3]\delta[E-E_2]P(e)de,$$

where

$$E_3=\frac{27\hbar\omega_0G_{11}}{4\lambda}(e_{xx}+e_{yy}-2e_{zz}).$$

A simple estimate of the effective width of the distribution is given by

$$W(\nabla)=\frac{1}{P(0,E)}\int P(\nabla,E)d\nabla.$$

Using methods similar to those applied in Appendix 2, one can calculate $W(\nabla)$. The result is,

$$W=\left(\frac{27\pi\hbar^2\omega_0^2E}{192\lambda G_{11}}\right)\times\frac{\int_0^1 dy\,H(b/y)/[y^2(1-y)^{1/2}(1-y+a)]}{\int_0^1 dy\,H(b/y)/[y(1-y)^{1/2}(1-y+a)(1-y+4a)]}.$$

One finds that the ratio of the two integrals has the asymptotic values $4a$ for a, $b\to\infty$ and $6a$ for a, $b\to 0$. Since both extremes of energy shift E give nearly the same value of $W(\nabla)$ and it is reasonable that the case $E\simeq 1$ will not give a very different result, one is justified in setting

$$W=\frac{27\pi\hbar\omega_0G_{11}\Delta}{16\lambda}.$$

In addition to having a numerical estimate of the width of the new strain mechanism, one has the following results: The width of the broadening mechanism is very nearly the same for all parts of the HFL (or DQL). The strain-broadening mechanism produces a linewidth that increases directly with increasing frequency.

APPLICATION OF g DISTRIBUTION WIDTH MECHANISM TO HFL

Assume that the broadening caused by the distribution of g values has a Lorentzian probability distribution. This is a reasonable approximation because this

width mechanism is linear in strain and because the strain distributions are Lorentzian. If one forms the convolution integral of the two strain width mechanisms, the g distribution broadened HFL shape will be given by,

$$I^*(E)_{\rm hf}=W\int_0^\infty \frac{I(E')_{\rm hf}dE'}{(E-E')^2+W^2}.$$

With the available spectrometer frequencies one finds experimentally that this broadening mechanism, in terms of half-height widths of resonance lines, never gives contributions appreciably greater than the low-frequency strain-broadening mechanism. It is therefore of value to express the g shift broadening in terms of a more sensitive parameter for which the mechanism causes large relative changes at lower frequencies. A sensitive parameter to use in observing broadening mechanisms is the width of the sharp or high-field side of the HFL derivative between the $\frac{1}{4}$ and $\frac{3}{4}$ height points. Call this quantity W_L. If the line is broadened only by the low-frequency strain mechanism, one has the relationship, $W_L=0.08W_{\rm hf}$, which can be obtained from Fig. 4 graphically. This formula is a good approximation whatever the value of a/b because the line shape is nearly independent of the ratio. Using Eq. (4) for the half-height width $W_{\rm hf}$, one has,

$$W_L=0.48\left(\frac{64G_{11}^2\Delta^2}{9\hbar\omega_0}\right)\left(\frac{b}{a}\right)^{0.84}$$

as the low-frequency asymptotic value. In the high-frequency limit the HFL shape is given by the expression,

$$I^*(E)_{\rm hf}\rightarrow\frac{27\hbar\omega_0G_{11}\Delta}{16\lambda}\left[E^2+\left(\frac{27\pi\hbar\omega_0G_{11}\Delta}{16\lambda}\right)\right]^{-1}.$$

From this one can show that what corresponds to W_L is

$$W_L=27\pi\hbar\omega_0G_{11}\Delta/16\lambda.$$

If one sets the low-frequency asymptotic expression for W_L equal to the high-frequency asymptotic expression, a condition for the minimum value of W_L is obtained. Thus,

$$\hbar^2\omega_0^2/\lambda G_{11}\Delta=0.64(b/a)^{0.84}. \quad (7)$$

This equation indicates that the frequency at which W_L is a minimum is directly proportional to the magnitude of the strains in a crystal. It is also evident that the ratio a/b must be determined before this relationship can be utilized.

In using the above method to determine the frequency of the minimum value of W_L, it has been tacitly assumed that the curve of W_L versus frequency on a log-log plot is symmetrical about the minimum value. Because the function $I(E)_{\rm hf}$ is complicated, it is not obvious that this is the case. However, using Fig. 5 one can obtain values of W_L versus frequency and show, within

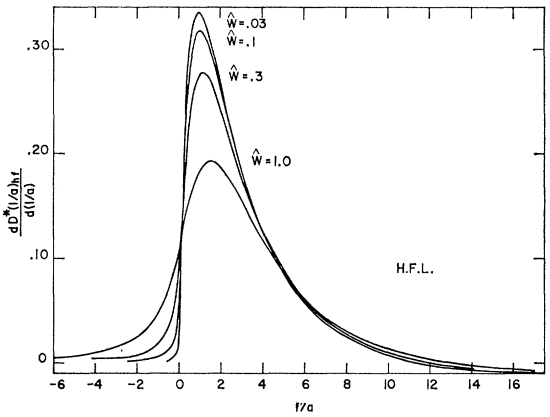

FIG. 5. The HFL shape broadened by the g distribution mechanism. Several ratios of the broadening parameter are shown.

graphical errors, that the curve is in fact symmetrical and that it has to a good approximation the form $W_L=s(t+\omega^2)/\omega$, where the constants s and t can be determined from the asymptotic limits of W_L.

COMPUTER PROGRAM FOR g DISTRIBUTION BROADENED LINE SHAPES

To obtain the "broadened" line shapes, a computer program has evaluated the function $I^*(E)_{\rm hf}$ and $I^*(E)_{\rm dq}$ as a function of E, for various values of the broadening parameter $\hat{W}$. The results have been plotted in curve form and are illustrated in Figs. 5 and 6.

The curves plot the derivative functions

$$\frac{dD^*(1/a)_{\rm hf}}{d(1/a)} \quad \text{and} \quad \frac{dD^*{}_1(1/a_1)_{\rm dq}}{d(1/a)},$$

where

$$D^*\left(\frac{1}{a}\right)_{\rm hf}=\frac{\hat{W}}{\pi}\int_0^\infty\frac{D(1/a')_{\rm hf}d(1/a')}{[(1/a)-(1/a')]+\hat{W}^2},$$

$$D_1{}^*\left(\frac{1}{a_1}\right)_{\rm dq}=\frac{\hat{W}_1}{\pi}\int_0^\infty\frac{D_1(1/a_1')_{\rm dq}d(1/a_1')}{[(1/a_1)-(1/a_1')]+\hat{W}_1{}^2},$$

in terms of the dimensionless variables $1/a$ and $1/a_1$, where $\hat{W}$ and $\hat{W}_1$ represent the broadening parameter width in units of $1/a$ and $1/a_1$, respectively, and where

$$I^*(E)_{\rm hf}=\frac{4}{3}\frac{(g\beta H_{\rm rf})^2}{\hbar}\frac{16}{3\pi^3}\tau D^*\left(\frac{1}{a}\right)_{\rm hf},$$

$$I^*(E)_{\rm dq}=8\hbar\omega_0(g\beta H_{\rm rf})^2T_1\tau\left(\frac{6}{\pi^2\epsilon n}\right)D_1{}^*\left(\frac{1}{a_1}\right)_{\rm dq},$$

and

$$D\left(\frac{1}{a}\right)_{\rm hf}=ba^{1/2}\int_0^1\frac{dy\,H(b/y)}{y(1-y+a)(1-y)^{1/2}},$$

$$D_1\left(\frac{1}{a_1}\right)_{dq}=b_1a_1^{1/2}\int_0^1\frac{dy\,H(b_1/y)}{y^2(1-y)^{1/2}(1-y+4a_1)(1-y+a_1)}.$$

EXPERIMENTAL RESULTS

Strain as a Line-Shape Mechanism

A simple check on the assumption of strain broadening is to compare the strain-broadened SQL width with the strain-broadened width of another ion species present as an impurity in the crystal. It has been shown that the energy shift of the SQL in the presence of strains is

$$\Delta E_{\mathrm{SQL}}=\tfrac{3}{4}G_{11}^{\mathrm{Fe}}(e_{xx}+e_{yy}-2e_{zz})$$

if the magnetic field is along the [100] crystal axis. Correspondingly, by using the same method and the same crystal orientation relative to the magnetic field, it can be shown that the energy shift of the Mn^{++} ($\frac{1}{2}$ to $\frac{3}{2}$ transition) is given by

$$\Delta E_{\mathrm{Mn}}=\tfrac{3}{2}G_{11}^{\mathrm{Mn}}(e_{xx}+e_{yy}-2e_{zz}).$$

Mn^{++} has an $S=\frac{5}{2}$ effective spin ground state. If one assumes that the widths of the stochastic distributions of cartesian strain components are the same at both the Mn^{++} and the Fe^{++} sites, then, using Watkins'[2] or Shiren's[4] G values, one can show that the ratio of the Mn^{++} ($\frac{1}{2}-\frac{3}{2}$) linewidth to the SQL width is given by

$$W_{\mathrm{Mn}}/W_{\mathrm{SQL}}=0.00325.$$

The Mn^{++} ($\frac{1}{2},\frac{3}{2}$) and the Mn^{++} ($\frac{1}{2},-\frac{1}{2}$) widths were measured for samples in which the SQL widths were also known. The Mn^{++} ($\frac{1}{2},-\frac{1}{2}$) line is not broadened by strains and very likely its width is determined by dipolar broadening. Therefore the Mn^{++} ($\frac{1}{2},-\frac{1}{2}$) linewidth was subtracted from the Mn^{++} ($\frac{1}{2},\frac{3}{2}$) width and the difference, presumably due to strains, was plotted against the width of the SQL. The results of this plot are shown in Fig. 7. The agreement between the theoretical ratio of strain widths and the experimentally measured ratio is good.

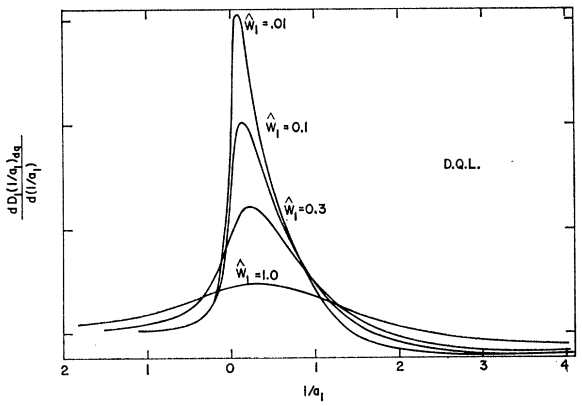

FIG. 6. The DQL shape broadened by the g distribution mechanism.

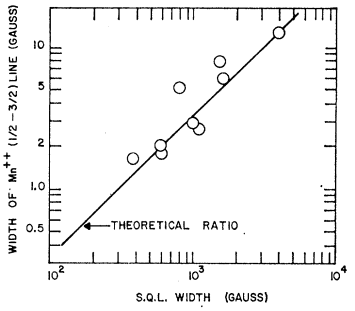

FIG. 7. Comparison of widths of Fe^{++} SQL and Mn^{++} ($\frac{1}{2}-\frac{3}{2}$) resonances. The magnetic field is along the (100) axis of the crystal. Each point corresponds to a different sample.

The theory of strain-induced line shapes predicts several relationships between the paramagnetic resonances of the Fe^{++} system. Some of these relationships will now be compared with experimental results.

Because the width of the HFL at low rf frequencies is a second-order perturbation of strain broadening, the width of the HFL is proportional to the square of the SQL width. This feature is verified by a comparison of the SQL and HFL widths measured at 9.5 Gc/sec and illustrated in Fig. 8.

Additional evidence is supplied by the detailed shape of the HFL. In Fig. 9 is shown a picture of the HFL resonance observed at 9.5 Gc/sec and at 4°K. This picture illustrates the low-frequency limit of strain-broadened line shape. If one subtracts off the baseline variation which is due to the SQL (see Fig. 1), and compares the resulting picture with the theoretical HFL shape shown in Fig. 5, the agreement is excellent.

One also finds experimentally that the width of the HFL varies inversely with the spectrometer frequency in the low-frequency limit. This feature is not illustrated.

The Ratio a/b

The width and height of the HFL are given in terms of the variables a and b, where

$$1/a=9E\hbar\omega_0/128G_{11}^2\Delta^2,\quad 1/b=E\hbar\omega_0/2G_{44}^2\delta^2.$$

Taking the average of Watkins' and Shiren's values of G_{11} and G_{44} quoted above, the ratio of a/b is given by $a/b=16(\Delta/\delta)^2$.

Equation (5) gives the ratio of the maximum height of the derivative of the HFL to the peak-to-peak height of the SGL. The quantity $I(E)_{\mathrm{hf}}m_{\mathrm{sq}}/I(E)_{\mathrm{sq}}m_{\mathrm{hf}}$ has been measured at 9 Gc/sec for about a dozen samples with the result,

$$I(E)_{\mathrm{hf}}m_{\mathrm{sq}}/I(E)_{\mathrm{sq}}m_{\mathrm{hf}}=2.0\pm0.3.$$

From this one has the estimate $a/b=13$.

Equation (6) gives the relationship between the HFL and SQL widths. From the graph of Fig. 8, which plots the HFL width against the SQL width for several samples at X band, one obtains

$$H_2w_{\mathrm{hf}}/w_{\mathrm{sq}}^2=0.16.$$

One therefore has the estimate $a/b=15$. Using the

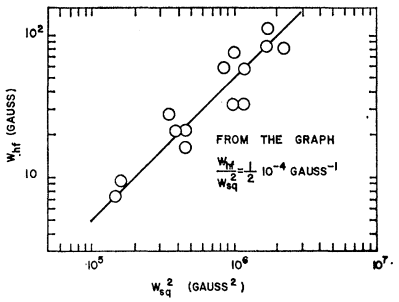

FIG. 8. Width of the HFL versus width squared of the SQL. Measurements were made at 9.5 Gc/sec. Each point corresponds to a different sample.

average value of a/b, $a/b=14$, one has the result,

$$\Delta/\delta=0.94\approx 1.$$

One intuitively expects $\Delta/\delta\approx 1$. The fact that this expectation has been substantiated is further evidence to support the strain-mechanism hypothesis of line shapes.

Evidence for the g Distribution Broadening Mechanism

In the theory of line shapes it was indicated that W_L has the form

$$W_L=s(t+\omega^2)/\omega.$$

If the plot of W_L versus frequency ω is made on a log-log scale, the shape of the curve, aside from translational shifting of position, is given by $(1+\omega^2)/\omega$. Experimentally the constants s and t are determined by moving this trial curve in a horizontal or vertical direction until it fits over the data points. This experimentally determined fit to the function is shown in Fig. 10. It is apparent that the width parameter W_L has a minimum in the neighborhood of 10 Gc/sec.

The broadening produced by the g distribution mechanism can be estimated from theory by using the measured values of the SQL width and the value of the ratio a/b. Using these values, the theoretical condition for the minimum of W_L, Eq. (7), becomes

$$\omega^2=0.28\ w_{sq},$$

where ω is the frequency in Gc/sec and w_{sq} is the peak-to-peak width of the SQL measured in gauss. This relationship also predicts, within the accuracy of the theory, that the minimum occurs near 10 Gc/sec.

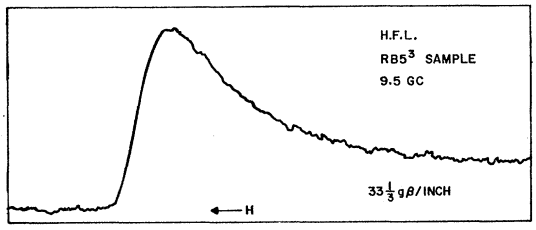

FIG. 9. The HFL derivative shape measured at 9.5 Gc/sec illustrating the low-frequency limit of strain broadening. Magnetic field increases to the left.

As additional evidence one has the following experimental information which can also be predicted from the theory.

The width parameter W_L measured at 72 Gc/sec, where the low-frequency strain mechanism gives an insignificant contribution to the width, correlates well with the SQL width, which is a measure of strain. The graph of W_L at 72 Gc/sec versus SQL width shown in Fig. 11 implies that these two widths are directly proportional to one another.

The width increase of W_L is directly proportional to spectrometer frequency. The RB1 sample in Fig. 10 illustrates this behavior.

The minimum of W_L decreases in frequency as the magnitude of strains in the crystal decreases. Compare the frequency of the minimum for the RB1 sample (Fig. 10), which has a SQL width of 400 G, with the RB5^4 samples for which the SQL width is about 1000 G.

Measurements on the width of the high field edge of the DQL also exhibit broadening as frequency is increased. Thus the width mechanism is not a pecularity of either the HFL or the SQL.

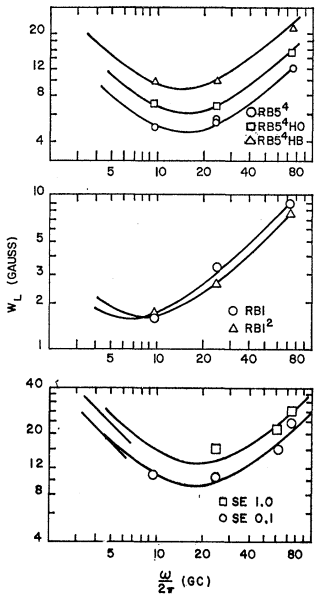

FIG. 10. The width W_L of the high-field edge of the HFL as a function of spectrometer frequency for several samples.

CONCLUSIONS

The theory of strain broadening of the Fe^{++} resonances using a model of stochastic distribution of Cartesian strain components at the paramagnetic ion sites gives only one adjustable parameter, the ratio a/b. Even this parameter is not completely arbitrary because it is proportional to the ratio of diagonal to off-diagonal strain-distribution widths, which one intuitively expects to be about unity. Experimental results quantitatively verify the applicability of this theory in many essential details. There is little doubt that strains in the crystal field potential cause the

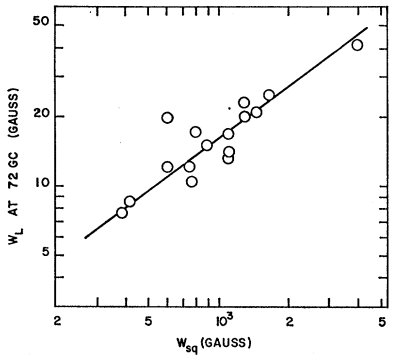

FIG. 11. The width parameter W_L at 72 Gc/sec versus SQL width. Each point corresponds to a different sample.

observed Fe^{++} paramagnetic resonance line shapes both at low frequencies and at high frequencies, for which cases two different strain-broadening mechanisms are operative.

ACKNOWLEDGMENTS

The author wishes to acknowledge the many helpful discussions that he had with Dr. R. H. Silsbee of the Physics Department at Cornell University.

APPENDIX 1

Density Matrix Approach to the DQL

The treatment of the DQL in terms of second-order rf field perturbation theory is complicated by the presence of the SQL transition. Since contribution to the DQL occurs for the case of little or no first-order strain shifts, the energy denominator encountered in second-order perturbation theory becomes vanishingly small, making the perturbation expression arbitrarily large. For this reason perturbation theory is not valid and the density matrix approach is used.

The energy differences of the 3 levels of the ground state in an applied magnetic field which produces the Zeeman splitting $\hbar\omega_0$, subjected to the first-order strain shift $\hbar\omega_1$, and the second-order strain shift $\hbar\omega_2$, can be taken to be

$$\omega_{12}=\omega_0+\omega_1+\omega_2,$$
$$\omega_{23}=\omega_0-\omega_1+\omega_2 \quad \omega_{13}=2\omega_0+2\omega_2.$$

The time variation of the density matrix is given by

$$\hbar\dot{\rho}_{nm}-i[\mathcal{H},\rho_{nm}],$$

where n and m vary over the levels 1, 2, and 3.

The static magnetic field part of the Hamiltonian is

$$\mathcal{H}_{nm}=gbH_0\delta_{nm}=E_n\delta_{nm}$$

and the rf magnetic field interaction is

$$\mathcal{H}_{nm}=gbH_{nm}e^{-i(\Omega_{nm}t+\phi_{nm})}\equiv V_{nm},$$

where Ω_{nm} and ϕ_{nm} are the frequencies and phases of the rf fields. The relaxation of the diagonal and off-diagonal density matrix components are treated in the usual phenomenological fashion by setting,

$$(\rho_{nn})_{\text{relax}}=1/T_1\sum_k(\rho_n\rho_{kk}-\rho_k\rho_{nn}),$$

$$(\rho_{nm})_{\text{relax}}=(1/T_2)\rho_{nm}, \quad n\neq m.$$

The components of the density matrix with a single subscript denote thermal equilibrium values in the absence of the rf field. This formulation includes the principle of detailed balancing and assumes, for simplicity, that all of the diagonal relaxation times are the same, T_1, and that all of the off-diagonal relaxation times are the same, T_2. By assuming only one value of T_1, the resulting expression will be altered only in the limit of saturation. The density-matrix equations can then be written as

$$\dot{\rho}_{nn}=(1/T_1)\sum_k(\rho_n\rho_{kk}-\rho_k\rho_{nn})+(1/i\hbar)\sum_k(V_{nk}\rho_{kn}-\rho_{nk}V_{kn}),$$

$$\dot{\rho}_{nm}=-(1/T_2)\rho_{nm}+(1/i\hbar)(E_n-E_m)\rho_{nm}+(1/ih)\sum_k(V_{nk}\rho_{km}-\rho_{nk}V_{km}), \quad n\neq m.$$

Following Clogston,[6] one makes in succession the substitutions,

$$\rho_{nm}=\sigma_{nm}e^{-i\omega_{nm}t}+\rho_{nm}^0, \quad \text{where} \quad \omega_{nm}=\hbar^{-1}(E_n-E_m)$$

$$\sigma_{nk}=\lambda_{nk}e^{-i(\Omega_{nk}-\omega_{nk})t}, \quad \text{with} \quad A_{nk}=\frac{gbH_{nk}}{2\hbar}e^{i\phi_{nk}}.$$

Keeping only the secular terms, the result is

$$0=\sum_k(\rho_n\lambda_{kk}-\rho_k\lambda_{nn})+iT_1\sum_k(A_{nk}\lambda_{kn}-\lambda_{nk}A_{kn})$$

$$1+iT_2(w_{nm}-\Omega_{nm})=iT_2\sum_k(A_{nk}\lambda_{km}-\lambda_{nk}A_{km}), \quad n\neq m.$$

In the case of the DQL and SQL transitions there is only one applied rf field so that one can set,

$$A_{12}=A_{23}=(gbH_{\text{rf}}/2\hbar)\equiv A, \quad A_{13}=0, \quad \Omega_{12}=\Omega_{23}\equiv\Omega.$$

These conditions correspond to the application of an rf field which is near resonance for the SQL and DQL.

One can further simplify the subsequent expressions by making the substitutions,

$$[1+iT_2(\omega_{12}-\Omega)]\equiv\alpha,$$
$$[1+iT_2(\omega_{13}-2\Omega)]\equiv\beta,$$
$$[1+iT_2(\omega_{23}-\Omega)]\equiv\gamma.$$

The equations of the six independent components of

[6] A. M. Clogston, Phys. Chem. Solids 4, 271 (1958).

the density matrix are then

$$\rho_1(\lambda_{22}+\lambda_{33})-(\rho_2+\rho_3)\lambda_{11}+iAT_1(\lambda_{21}-\lambda_{12}), \quad \text{(A1)}$$

$$\rho_2(\lambda_{11}+\lambda_{33})-(\rho_1+\rho_3)\lambda_{22}+iAT_1[(\lambda_{12}-\lambda_{21})+(\lambda_{32}+\lambda_{23})], \quad \text{(A2)}$$

$$\rho_3(\lambda_{11}+\lambda_{22})-(\rho_1+\rho_2)\lambda_{33}+iAT_1(\lambda_{23}-\lambda_{32}), \quad \text{(A3)}$$

$$\alpha\lambda_{12}=iAT_2[(\lambda_{22}-\lambda_{11})-\lambda_{13}],$$

$$\beta\lambda_{13}=iAT_2(\lambda_{23}-\lambda_{12}),$$

$$\gamma\lambda_{23}=iAT_2(\lambda_{33}-\lambda_{22}+\lambda_{13}).$$

The rf power absorbed per spin is equal to the amount of power dissipated through spin-lattice relaxation. This is given by,

$$R=gbH_0[(\lambda_{33}-\lambda_{11})-(\rho_3-\rho_1)].$$

By solving the 6 simultaneous equations for the components of the density matrix to get λ_{11} and λ_{33}, and substituting the expressions for these quantities into equation, the absorbed power per spin is

$$R=\frac{gbH_0\tau S}{3T_1}\left[\frac{(P+Q+4N)+6S(PQ+PN+QN)}{1+2S(P+Q+N)+3S^2(PQ+PN+QN)}\right]$$

where $\tau=gbH_0/kT$ is the Boltzmann factor, $S=A^2T_1T_2$ is the saturation factor, and where

$$N\equiv A^2T_2^2\left[\frac{\alpha\beta\gamma+\alpha^*\beta^*\gamma^*+4A^2T_2^2}{|\alpha\beta\gamma+A^2T_2^2(\alpha+\gamma)|^2}\right],$$

$$P\equiv\frac{2|\beta\gamma|^2+A^2T_2^2[(\alpha+\gamma)\beta^*\gamma^*+(\alpha^*+\gamma^*)\beta\gamma]}{|\alpha\beta\gamma+A^2T_2^2(\alpha+\gamma)|^2},$$

$$Q\equiv\frac{2|\beta\alpha|^2+A^2T_2^2[(\alpha+\gamma)\alpha^*\beta^*+(\alpha^*+\gamma^*)\alpha\beta]}{|\alpha\beta\gamma+A^2T_2^2(\alpha+\gamma)|^2}.$$

Redfield[7] has discussed the effects of saturation on the Bloch and hence on the density matrix theory. He indicates that the use of the phenomenological quantities T_1 and T_2 is not a good assumption if $S\gtrsim 1$, and for this reason the validity of the above equations in the limit of saturation is questionable.

If one uses the intensity behavior with rf power to discriminate between the terms producing the SQL and DQL, one finds that parts of the terms P and Q vary as the rf field squared and are responsible for the SQL. For the unsaturated case one has

$$R_{sq}=\frac{gbH_0S\tau}{3T_1}\left[\frac{2}{|\alpha|^2}+\frac{2}{|\gamma|^2}\right].$$

If one sums over ω_1, one need not distinguish between the resonating denominator factors $|\alpha|^2$ and $|\gamma|^2$. Picking out the terms which vary as the fourth power of the rf field strength as the source of the DQL, the result for usual the case of $T_2\ll T_1$ is

$$R_{dq}=\frac{8gbH_0\tau S^2}{T_1}\left[\frac{1}{|\alpha\gamma|^2}\right].$$

In a similar manner one can apply the density matrix method to calculate the power absorbed per spin for the HFL transition. If the HFL is not saturated, the result is

$$R_{hf}=\left(\frac{4gbH_0S'\tau}{3T_1'}\right)\left(\frac{8(e_{xz}^2+e_{yz}^2)}{\hbar^2\omega_0^2}\right)\left[\frac{1}{1+(\omega+\omega_2)^2T_2^2}\right],$$

where $S'=g^2b^2H_x^2T_1'T_2$ and T_1' is the $\Delta M=2$ spin-lattice relaxation time.

APPENDIX 2

Calculation of Strain-Induced Line Shapes

As an example of this calculation, the HFL will be used. Calculations for the SQL and DQL shapes proceed in an analogous fashion.

Using the results of Appendix 1 and assumptions quoted in the text, the intensity of the HFL (aside from some constant factors) is given by

$$I(E)=\frac{8G_{44}^2}{\hbar^2\omega_0^2}\int_{-\infty}^{\infty}\cdots\int(e_{xz}^2+e_{yz}^2)\,\delta\left[E-\frac{2G_{44}^2}{\hbar\omega_0}(e_{xy}^2+e_{xz}^2+e_{zx}^2)-\frac{9}{8}\frac{G_{11}^2}{\hbar\omega_0}(e_{xx}-e_{yy})^2\right]$$
$$\times\left(\frac{\delta}{\pi}\right)^3\left(\frac{\Delta}{\pi}\right)^3\frac{de_{xx}}{(e_{xx}^2+\Delta^2)}\frac{de_{yy}}{(e_{yy}^2+\Delta^2)}\frac{de_{xy}}{(e_{xy}^2+\delta^2)}\frac{de_{yz}}{(e_{yz}+\delta^2)}\frac{de_{zx}}{(e_{zx}^2+\delta^2)}.$$

E represents the energy shift from the unstrained Zeeman splitting. Make the following substitutions:

$$=\hat{E}\frac{E\hbar\omega_0}{2}, \quad e_{xy}=\frac{u}{G_{44}}, \quad e_{yz}=\frac{v}{G_{44}}, \quad e_{zx}=\frac{w}{G_{44}},$$

$$e_{xx}=\frac{3}{4}\frac{x}{G_{11}}, \quad e_{yy}=\frac{3}{4}\frac{y}{G_{11}}, \quad G_{44}=n, \quad \tfrac{4}{3}G_{11}=\epsilon.$$

Then, since aside from the factor $e_{xz}^2+e_{yz}^2$, the integral is symmetric in e_{xy}, e_{yz}, e_{zx}, one gets

$$I(\hat{E})=\frac{8}{3\hbar\omega_0}\left(\frac{n}{\pi}\right)^3\left(\frac{\epsilon}{\pi}\right)^3\int\cdots\int\frac{(u^2+v^2+w^2)dudvdw}{(u^2+n^2)(v^2+n^2)(w^2+n^2)}$$
$$\times\frac{dxdy}{(x^2+\epsilon^2)(y^2+\epsilon^2)}\delta[\hat{E}-(u^2+v^2+w^2)-(x-y)^2].$$

[7] A. R. Redfield, Phys. Rev. 98, 1787 (1955).

This can be written in the form

$$I(\hat{E})=\frac{8}{3\hbar\omega_0}\int_0^{\hat{E}}F(\hat{E}_1)G(\hat{E}-\hat{E}_1)d\hat{E}_1,$$

where

$$F(\hat{E}_1)=\iiint\left(\frac{n}{\pi}\right)^3\times\frac{(u^2+v^2+w^2)dudvdw\delta[\hat{E}_1-(u^2+v^2+w^2)]}{(u^2+n^2)(v^2+n^2)(w^2+n^2)},$$

$$G(\hat{E}_2)=\left(\frac{\epsilon}{\pi}\right)^2\iint\frac{dxdy}{(x^2+\epsilon^2)(y^2+\epsilon^2)}\delta[\hat{E}_2-(x-y)^2].$$

Changing the first integral to "spherical coordinates," the result is,

$$F(\hat{E}_1)=\left(\frac{n}{\pi}\right)^3\iiint\frac{r^4dr\sin\theta d\theta d\phi\delta(\hat{E}_1-r^2)}{(r^2\cos^2\theta+n^2)(r^2\sin^2\theta\cos^2\phi+n^2)(r^2\sin^2\theta\sin^2\phi+n^2)}.$$

Eliminating the δ function,

$$F(\hat{E}_1)=\frac{1}{2}\left(\frac{n}{\pi}\right)^3\int_0^{\pi}\frac{\hat{E}_1^{3/2}\sin\theta d\theta}{(\hat{E}_1\cos^2\theta+n^2)}\times\int_0^{2\pi}\frac{d\phi}{(\hat{E}_1\sin^2\theta\sin^2\phi+n^2)(\hat{E}_1\sin^2\theta\cos^2\phi+n^2)}.$$

Doing the ϕ integral,

$$F(\hat{E}_1)=2\left(\frac{n}{\pi}\right)^2\hat{E}_1^{3/2}\times\int_0^{\pi}\frac{\sin\theta d\theta}{(\hat{E}_1\cos^2\theta+n^2)(\hat{E}_1\sin^2\theta+2n^2)(\hat{E}_1\sin^2\theta+n^2)^{1/2}}.$$

Let $x=\cos\theta$. Then,

$$F(\hat{E}_1)=4\hat{E}_1^{3/2}\left(\frac{n}{\pi}\right)^2\int_0^1\frac{dx}{\hat{E}_1x^2+n^2}\times\frac{1}{(\hat{E}_1-\hat{E}_1x^2+n^2)^{1/2}}\frac{1}{(\hat{E}_1-\hat{E}_1x^2+2n^2)}.$$

It is not possible to simplify this expression further.

In solving for the integral G, let $p=x-y$, $q=x+y$. Since the Jacobian of the transformation is $\frac{1}{2}$, the result is

$$G(\hat{E}_2)=8\left(\frac{\epsilon}{\pi}\right)^2\iint\frac{dp\,dq(\hat{E}_2-p^2)}{[(q+p)^2+4\epsilon^2][(q-p)^2+4\epsilon^2]}.$$

Eliminating the δ function and contour integrating, one has,

$$G(\hat{E}_2)=\frac{1}{2\hat{E}_2^{1/2}}\left(\frac{2\epsilon}{\pi}\right)\frac{1}{\hat{E}_2+4\epsilon^2}.$$

Substituting the expressions for G and F into $I(E)$ and letting $y=\hat{E}_1/\hat{E}$, $a=(2\epsilon)^2/\hat{E}$, $b=n^2/\hat{E}$, $b/y=n^2/\hat{E}_1$, the final result is

$$I(E)=\frac{16}{3\pi^3}\frac{ba^{1/2}}{\hbar\omega_0}\int_0^1\frac{dyH(b/y)}{y(1-y+a)(1-y)^{1/2}}$$

$$H(b/y)=\int_0^1\frac{dx}{[x^2+(b/y)][1-x^2+(b/y)]^{1/2}[1-x^2+(2b/y)]},$$

where

$$a=\frac{128G_{11}^2\Delta^2}{9\hbar\omega_0E},\quad b=\frac{2\delta^2G_{44}^2}{\hbar\omega_0E}.$$